

sensor package with a 2 mm-diameter/10-turn (226 nH with Q of 23 at 40 MHz) sensing coil sandwiched between the PCB and the sensor package bottom plate exhibiting a thickness of 80 μm . It should be noted that for the initial study the prototype design is powered by an external DC power supply to ensure a stable oscillator frequency. The sensor package is then filled with PDMS to seal the electronic components, followed by a 10 μm Parylene C coating serving as a biocompatible and moisture resistant layer. A 3 mm x 3 mm x 400 μm functionalized hydrogel slab embedded with a 3 mm x 3 mm x ~ 80 μm metallic sensing plate is adhered onto a 3D-printed adjustable platform via a gelbond film. The adjustable platform is then assembled to the 3D-printed sensor package by using screws, which can adjust the gap size between the metallic sensing plate and the package bottom plate to approximately 50 μm as shown in the figure. A small gap size is critical to achieve a high sensitivity. The assembled sensor is then immersed into 1xPBS solution with a controlled glucose level for characterization. The glucose concentration can alter the sensing coil inductance, which in turn modulates the oscillator frequency to be detected by a nearby receiver.

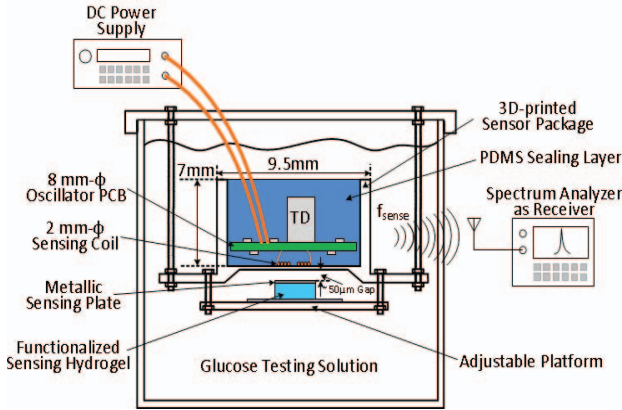


Fig. 2. DC-powered *In vitro* wireless glucose sensor test setup.

Figure 3 presents a tunnel diode oscillator-based sensor design topology, where a commercial silicon tunnel diode is employed for the prototype demonstration.

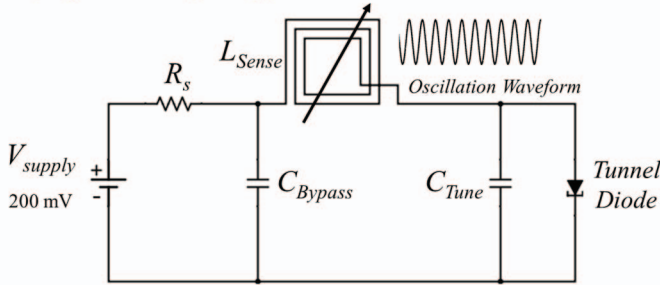


Fig. 3. DC-powered tunnel diode oscillator-based sensor topology.

The tunnel diode is biased at 200 mV to achieve a negative resistance of around -1200Ω , sufficient to compensate the LC tank loss. The oscillator dissipates a low DC power of 40 μW while developing -19 dBm RF power. Figure 4 shows a typical oscillator output power spectrum, exhibiting a -78 dBm power at 37.96 MHz, received by a receiver positioned at approximately 4 cm away from the sensor module.

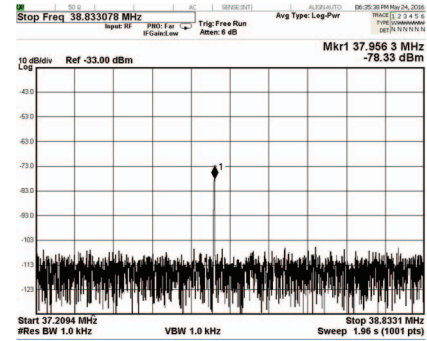


Fig. 4. Wirelessly received oscillator output power spectrum.

III. GLUCOSE CHARACTERIZATION

The glucose characterization was performed using the test setup depicted in Figure 2. The sensor was first immersed in 1xPBS solution with a glucose concentration of 4 mM (close to that of human blood) to reach an equilibrium. The concentration was then dropped to 0 mM and remained unchanged for three days to exam the oscillator frequency stability, which exhibited a 5 kHz/day drift from the 24th to the 72nd hour. At this point, the glucose was ramped to 10 mM with a 2 mM step change every 24 hours. The measurement result is plotted in Figure 5.

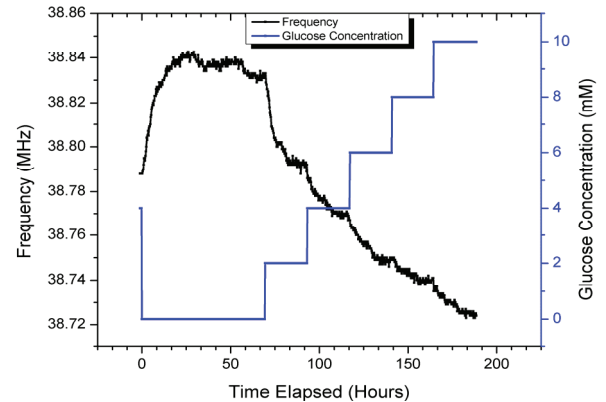


Fig. 5. Glucose test results using the DC-powered wireless sensor.

The sensor exhibited a sensitivity of 20 kHz/mM when the glucose concentration was below 2 mM. The sensitivity was reduced to 8.5 kHz/mM when the glucose concentration was increased to 10 mM, likely due to hydrogel saturation. Based on the measured frequency drift, a glucose sensing accuracy of approximately 0.2 mM at lower concentration and 0.6 mM at higher concentration, respectively, can be determined.

IV. RF-POWERED WIRELESS GLUCOSE SENSOR DESIGN

It is highly attractive to develop a fully wireless glucose sensor for future implantable applications. Consequently, the feasibility of an RF-powered wireless tunnel diode oscillator-based glucose sensor was explored. Figure 6 depicts the *in vitro* experimental setup for the proposed feasibility study, which leverages the design and packaging principle presented in Figure 2. Instead of powering the sensor module with a DC power supply, an RF powering scheme is employed, where a 2 cm-diameter/10-turn RF power transmitting coil (4.3 μH with

Q of 73 at 2 MHz) is positioned over an 8 mm-diameter/10-turn RF power receiving coil ($1.3 \mu\text{H}$ with Q of 25 at 2 MHz) sealed inside the sensor package with a separation distance of approximately 2 cm.

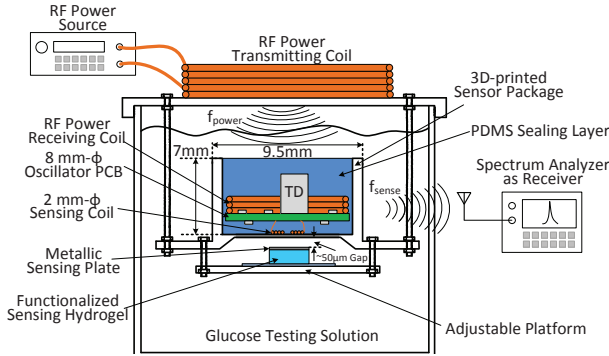


Fig. 6. RF-powered *In vitro* wireless glucose sensor test setup.

Figure 7 presents the RF-powered wireless tunnel diode oscillator-based sensor design, where a pair of tuned LC tank circuits is used to couple an external RF power source to energize the sensor module. The RF powering frequency is chosen at 2 MHz so that the circuit achieves a highest/optimal power transfer efficiency. A clamping diode is introduced after the rectifier diode with an objective to achieve a stable output DC voltage around 200 mV to bias the tunnel diode. The clamping diode dissipates a DC power of $60 \mu\text{W}$, thus resulting in an overall oscillator power dissipation of $100 \mu\text{W}$. An external RF power of 41 mW is required to operate the wireless sensor module.

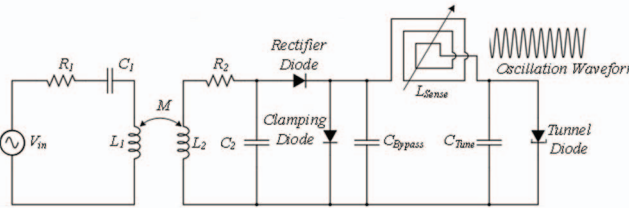


Fig. 7. RF-powered tunnel diode oscillator design topology.

The RF-powered wireless glucose sensor assembly process and test setup are illustrated in Figure 8. A similar procedure was employed for the sensor package and glucose characterization described in Section II. It should be noted that the current system form factor can be greatly minimized by employing integrated electronics and optimizing the sensor package housing the functionalized hydrogel slab. Long-term oscillator frequency stability under RF powering was investigated over 65 hours. The measured result shows that the oscillator frequency exhibits a significant drift over time, which was not observed from the previous stability test using a DC power supply. A further analysis reveals the frequency drift exhibits a periodicity of approximately 24 hours, which could be caused by environment changes such as temperature and electric load conditions. A robust voltage regulator is, therefore, planned to replace the clamping diode to achieve a more stable DC output bias voltage for the tunnel diode, thus expecting an improved frequency stability. Other techniques

employing FSK modulation and reference oscillator will also be explored for a robust data communication.

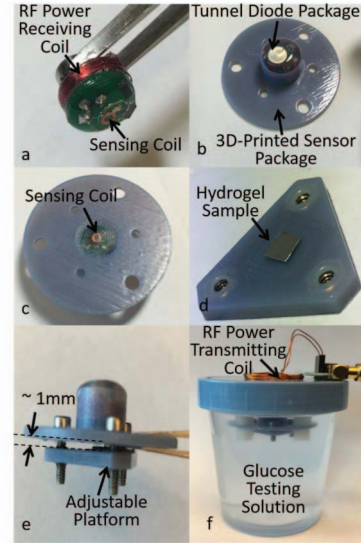


Fig. 8. Photos of RF-powered wireless glucose sensor assembly and test setup. (a) Tunnel diode oscillator PCB with RF power receiving coil; (b) Oscillator PCB placed inside 3D-printed sensor package sealed with PDMS; (c) Bottom view of the 3D-printed sensor package showing the sensing coil; (d) 3D-printed adjustable platform holding the functionalized hydrogel sample embedded with a metallic sensing plate; (e) Assembled wireless glucose sensor module; (f) Assembled sensor module in glucose testing container.

V. CONCLUSIONS

A wireless hydrogel-based glucose sensor employing an inductive sensing technique has been demonstrated for future implantable applications. The prototype system under a stable DC supply is capable of sensing and wirelessly transmitting glucose information within the human physiological range. Future research effort will be devoted to improving frequency stability under RF-powering condition as well as shortening the response time of the glucose-sensitive hydrogel.

ACKNOWLEDGMENT

This research is supported by the National Science Foundation under grant number: ECCS-1408265.

P. Tathireddy has commercial interest in Applied Biosensors, LLC.

REFERENCES

- [1] S. A. Zotov, *et al.*, "Folded-MEMS-Pyramid Inertial Measurement Unit," *IEEE Sensors Journal*, Vol.11, No.11, pp.2780-2789, 2011.
- [2] M. Lei, *et al.*, "Integration of Hydrogels with Hard and Soft Microstructures," *Journal of Nanoscience and Nanotechnology*, Vol. 7, 2007, pp. 780-789.
- [3] N. S. Oliver, *et al.*, "Glucose sensors: a review of current and emerging technology," *Diabetic Medicine*, December, pp. 1464-5491, 2008.
- [4] P-H Kuo, *et al.*, "A Hydrogel-Based Implantable Wireless CMOS Glucose Sensor SoC," *IEEE International Symposium on Circuits and Systems*, Seoul, Korea, 2012, pp. 994-997.
- [5] Y. Yu, *et al.*, "Inductive Sensing Technique For Low Power Implantable Hydrogel-Based Biochemical Sensors," *IEEE Sensors Conf.*, 2015, pp 129 - 133.